EAST EUROPEAN JOURNAL OF PHYSICS. 4. 454-460 (2025)
DOI:10.26565/2312-4334-2025-4-46 ISSN 2312-4334

# DESIGN AND DEVELOPMENT OF FERRITE-TIO$_2$ NANOCOMPOSITES WITH TUNABLE MAGNETIC PROPERTIES

**Hanaa Sh. Ahmed[1], A.K. Sijo[2]*, Ali M. Mohammad[1#], Hero S. Ahmed Al-Jaf[1], Balen H. Ahmed[1], J. Mazurenko[3]**

[1]*University of Garmian, College of Education, Department of Physics, Kurdistan region, Kalar-46021, Iraq*
[2]*Department of Physics, Mary Matha Arts & Science College, Mananthavady, Kannur University-670645, India*
[3]*Department of Medical Informatics, Ivano-Frankivsk National Medical University, 2 Halytska Str., 76018, Ivano-Frankivsk, Ukraine*
*Corresponding Author e-mail: *aksijo@marymathacollege.ac.in; #alimustaf392@gmail.com*
Received August 14, 2025; revised October 2, 2025; accepted October 23, 2025

Ni-ferrite-TiO$_2$ nanocomposites with varying TiO$_2$ content (0%, 25%, 50% and 75%) were synthesized using the sol-gel auto-combustion method and characterized through XRD, FE-SEM, VSM, and Raman spectroscopy. The XRD analysis confirmed the coexistence of ferrite and TiO$_2$ phases. FE-SEM images revealed uniform particle distribution and a reduction in particle size as TiO$_2$ content increased. Raman spectroscopy showed strong TiO$_2$-related vibrational modes, with the highest intensity observed in the 75% TiO$_2$ sample, diminishing as TiO$_2$ content decreased. Peaks observed in pure Ni-ferrite (283, 402, 469 and 689 cm$^{-1}$) shifted to lower wavelengths with increasing TiO$_2$ doping, indicating altered vibrational modes due to phase interactions. These interactions likely contributed to changes in the magnetic properties. VSM analysis revealed a decrease in saturation magnetization and magnetic remanence with increasing TiO$_2$ content, while coercivity remained stable. The magnetic behavior was attributed to TiO$_2$ dilution and phase interfaces, offering valuable insights for the design of magnetic materials with customized properties.
**Keywords:** *Ferrite; Nanocomposites; Magnetic properties; Nanoparticles; Hybrid ferrite*
**PACS:** 75.75.+a ; - 81.16.-c

## 1. INTRODUCTION

The pursuit of advanced magnetic materials with tailored properties has become a central focus of modern technological innovation. Magnetic nanomaterials offer promising opportunities for applications in spintronics, magnetic storage, biomedical devices, and energy storage systems [1][2]. Among these, nickel ferrite (NiFe) nanoparticles stand out due to their remarkable magnetic characteristics, stability, and biocompatibility [3].

Ni ferrite nanoparticles are known for their excellent magnetic properties, such as high saturation magnetization and coercivity, making them suitable for various high-performance applications [4,5]. Moreover, the magnetic behavior of these nanoparticles can be further optimized by altering their composition, structure, and morphology [6]. Studies on similar ferrite-based nanocomposites, such as cobalt ferrite (CoFe) and zinc ferrite (ZnFe), have demonstrated distinct magnetic properties. CoFe nanoparticles exhibit high magnetic anisotropy and coercivity [7], while ZnFe nanoparticles are recognized for their magnetic stability and biocompatibility [8].

The potential of NiFe nanoparticles can be expanded through hybridization with other materials, creating multifunctional nanocomposites with enhanced magnetic and structural properties. Titanium dioxide (TiO$_2$) emerges as an excellent material for this purpose due to its unique optical, electrical, and magnetic properties [9]. Integrating TiO$_2$ with NiFe nanoparticles can yield nanocomposites with enhanced magnetic properties, improved thermal stability, and increased surface area [10].

In this study, Ni-ferrite-TiO$_2$ nanocomposites with varying TiO2 content were synthesized using the sol-gel auto-combustion method. This technique provides precise control over the composition, structure, and morphology of the nanocomposites, enabling a systematic investigation of how TiO$_2$ incorporation influences their magnetic properties [11]. Our research investigates the structural, morphological, and magnetic properties of NiFe-TiO$_2$ nanocomposites to gain a deeper understanding of the mechanisms underlying their enhanced magnetic behavior. The insights gained from this study will aid in the development of multifunctional nanomaterials with customized magnetic properties, opening new possibilities for applications in magnetic storage, spintronics, biomedical devices, and energy storage technologies.

## 2. Materials and methods

### 2.1 Synthesis

$NiFe_2O_4$ spinel nanoferrite was synthesized using a sol-gel auto-combustion method [12,13]. Stoichiometric amounts of analytical grade of ferric nitrate ($Fe(NO_3)_3 \cdot 9H_2O$), nickel nitrate ($Ni(NO_3)_2 \cdot 6H_2O$), and citric acid ($C_6H_8O_7$) were dissolved in deionized water, maintaining a 1:1 molar ratio [14]. The pH was adjusted to neutral (pH 7) by adding ammonia while stirring. The mixture was then heated to 90°C, forming a dense gel, which was subsequently heated to 275°C, initiating a combustion reaction that produced as-burnt ferrite powder. The powder was calcined at 500°C for 3

***Cite as:*** H.Sh. Ahmed, A.K. Sijo, A.M. Mohammad, H.S.A. Al-Jaf, B.H. Ahmed, J. Mazurenko, East Eur. J. Phys. 4, 454 (2025), https://doi.org/10.26565/2312-4334-2025-4-46

hours in air to remove organic residues and achieve a uniform particle size distribution [15]. To explore the impact of $TiO_2$ content on the nanocomposite properties, $TiO_2$ nanoparticles were introduced into the ferrite nanopowder at various ratios (0%, 25%, 50%, and 75%). The structural, morphological, and magnetic properties of the resulting ferrite-$TiO_2$ nanocomposites were comprehensively characterized.

### 2.2 Material characterization

The crystalline structure of the ferrite nanocomposites was examined using X-ray diffraction (XRD) analysis performed on a PANalytical X'pert Pro instrument (Netherlands) with a Cu Kα radiation source (λ = 1.54048 Å) [16]. The surface morphology of the nanoparticles was investigated using field emission-scanning electron microscopy (FE-SEM) with a MIRA3-XMU model (TESCAN, Czech Republic) [17]. Raman spectra using XploRa-HOBIBA with a 785 nm laser were employed to identify the spinel ferrite phase [18]. The magnetic properties of the ferrite nanocomposites were characterized at room temperature using a vibrating sample magnetometer (VSM) from LBKFB Meghnatis Daghigh Kavir Company, with an applied magnetic field ranging from -10 to +10 kOe [19].

## 3. RESULTS AND DISCUSSION

The XRD patterns of the $NiFe_2O_4/TiO_2$ nanocomposites with varying $TiO_2$ content (0%, 25%, 50%, and 75%) are presented in Figure 1. The FullProf-fitted spectra reveal well-defined peaks at (220), (311), (222), (400), (422), and (440), which are characteristic of the spinel ferrite phase [20]. These peaks confirm the presence of the $NiFe_2O_4$ spinel structure and indicate that the samples are free from detectable impurities [21]. In addition to the ferrite phase, the $TiO_2$ phase was identified through spectral fitting techniques [22]. The XRD patterns correspond well with known reference patterns for the cubic spinel phase of $NiFe_2O_4$ (JCPDS card no. 00-054-0964) and the tetragonal anatase phase of $TiO_2$ (JCPDS card no. 00-021-1272) [23]. The accurate matching of these patterns with standard reference cards validates the successful incorporation of $TiO_2$ into the $NiFe_2O_4$ matrix and confirms the preservation of the distinct crystal structures of both components within the nanocomposites. This indicates that $TiO_2$ is present in its anatase form and does not interfere with the spinel structure of the ferrite, thus allowing for the exploration of combined properties of these materials.

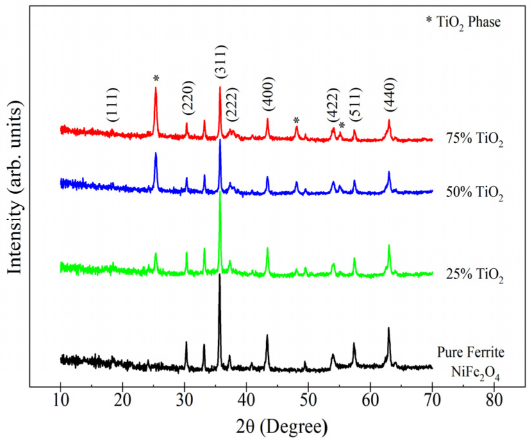


**Figure 1.** XRD patterns of 0%, 25%, 50%, and 75% $NiFe_2O_4/TiO_2$ nanocomposites

The structural parameters of the $NiFe_2O_4/TiO_2$ nano composites, determined through FullProf fitting, are summarized in Table 1. The crystallite size ($D_{XRD}$) and particle size ($D_{FE\text{-}SEM}$) values show a slight variation with increasing $TiO_2$ content. Specifically, a minimum crystallite size of 41.72 nm is observed for the 25% $TiO_2$ sample. This reduction in crystallite size can be attributed to the grain refinement effect induced by the incorporation of $TiO_2$. The presence of $TiO_2$ may disrupt the growth of $NiFe_2O_4$ grains, leading to smaller crystallite sizes [24]. The lattice parameter (a) values range from 5.347 Å to 7.213 Å, reflecting a subtle expansion of the crystal lattice with increasing $TiO_2$ content. This lattice expansion is likely due to the substitution of larger $Ti^{4+}$ ions for the smaller $Fe^{3+}$ ions in the $NiFe_2O_4$ lattice. As $Ti^{4+}$ ions are larger than $Fe^{3+}$ ions, their incorporation into the $NiFe_2O_4$ lattice increases the lattice dimensions, which is consistent with the observed increase in the lattice parameter [25].

**Table 1.** Structural Parameters from XRD & SEM analysis- crystallite size ($D_X$), particle size ($D_S$), lattice parameter (a), density ($\rho_X$), microstrain($\varepsilon$) and dislocation density ($\delta$)

| *$TiO_2$ %* | *$D_{XRD}$ (nm)* | *$D_{SEM}$ (nm)* | *a (Å)* | *$\rho_x$* | *$\varepsilon\times10^{-3}$* | *$\delta\times10^{15}$* |
|---|---|---|---|---|---|---|
| 0 | 44.85 | 17.9 | 8.350 | 5.35 | 1.5 | 0.599 |
| 25 | 41.72 | 19.9 | 8.335 | 7.21 | 1.91 | 0.824 |
| 50 | 45.01 | 22.1 | 8.333 | 7.21 | 1.80 | 0.720 |
| 75 | 49.08 | 21.9 | 8.335 | 7.21 | 1.61 | 0.591 |

The density ($\rho_x$) of the nanocomposites is found to be lowest for the 0% $TiO_2$ sample and remains relatively constant for the composites with higher $TiO_2$ content. This suggests that the addition of $TiO_2$ does not significantly alter the overall density of the nanocomposites. The lack of significant change in density might indicate that the $TiO_2$ particles are well-dispersed within the $NiFe_2O_4$ matrix, without causing substantial changes in the overall packing density of the material [25]. Additionally, the microstrain ($\varepsilon\times10^{-3}$) values decrease with increasing $TiO_2$ content, indicating a relaxation of the crystal structure. Microstrain is a measure of local lattice distortions and defects. The decrease in microstrain with higher $TiO_2$ content suggests that the incorporation of $TiO_2$ reduces lattice distortions and helps to relieve internal stresses within the $NiFe_2O_4$ lattice. This reduction in microstrain is likely due to the reduced lattice mismatch between the $NiFe_2O_4$ and $TiO_2$ phases, leading to a more coherent and less strained crystal structure [26].

The surface morphology of the $NiFe_2O_4/TiO_2$ nano composites was examined using field emission scanning electron microscopy (FESEM), with the resulting images presented in Figure 2a-d. The FESEM images provide detailed insights into the particle size, shape, and distribution of the nanocomposites. These images reveal that the nanoparticles exhibit a relatively uniform distribution across the sample, with variations in particle size that are dependent on the $TiO_2$ content. The observations from the FESEM analysis are crucial for understanding the impact of $TiO_2$ incorporation on the surface characteristics of the $NiFe_2O_4$ matrix, which can influence the material's overall performance in various applications [27].

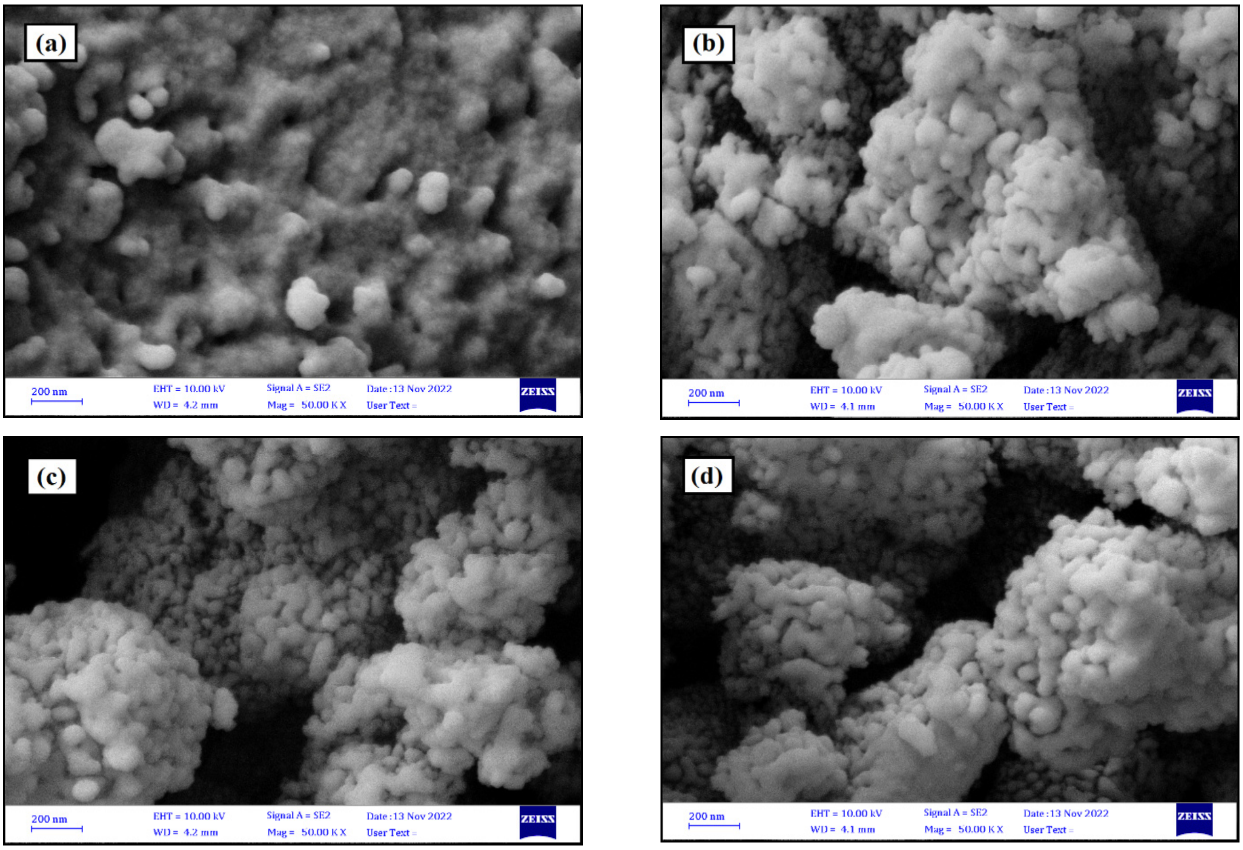


**Figure 2.** FE-SEM images of 0%, 25%, 50%, and 75% $NiFe_2O_4/TiO_2$ nanocomposites

The FE-SEM microstructural analysis (Figure 3a-d) revealed a nearly homogeneous particle size distribution across the surface, with particles predominantly exhibiting semi-spherical shapes. This analysis highlights the significant effect of $TiO_2$ doping on particle size, demonstrating that higher $TiO_2$ content (75%) results in noticeable particle enlargement. The microstructural examination provides detailed insights into the average size and grain growth characteristics, which are essential for understanding the material's physical, electrical, and magnetic properties. Particle agglomeration is evident, with smaller particles coalescing to achieve a lower free energy state, a trend that is more pronounced with increased $TiO_2$ doping. Additionally, there is a noticeable tendency for aggregation among numerous ferrite nanoparticles. The observed porous structures may result from substantial gas release during the combustion process, while the formation of agglomerated regions is likely due to the inherent interactions among magnetic nanoparticles [28].

The average crystallite size ($D_{XRD}$) and particle size ($D_{FE\text{-}SEM}$) show a significant dependence on $TiO_2$ content, as summarized in Table 1. The images also indicate that the particle sizes of the two phases vary with the relative content of each component. As $TiO_2$ content increases, the size of the nanocomposite particles also increases. Uniform structures are observed in the intermediate compositions, suggesting coherent grain growth within the constituent phases of the composites.

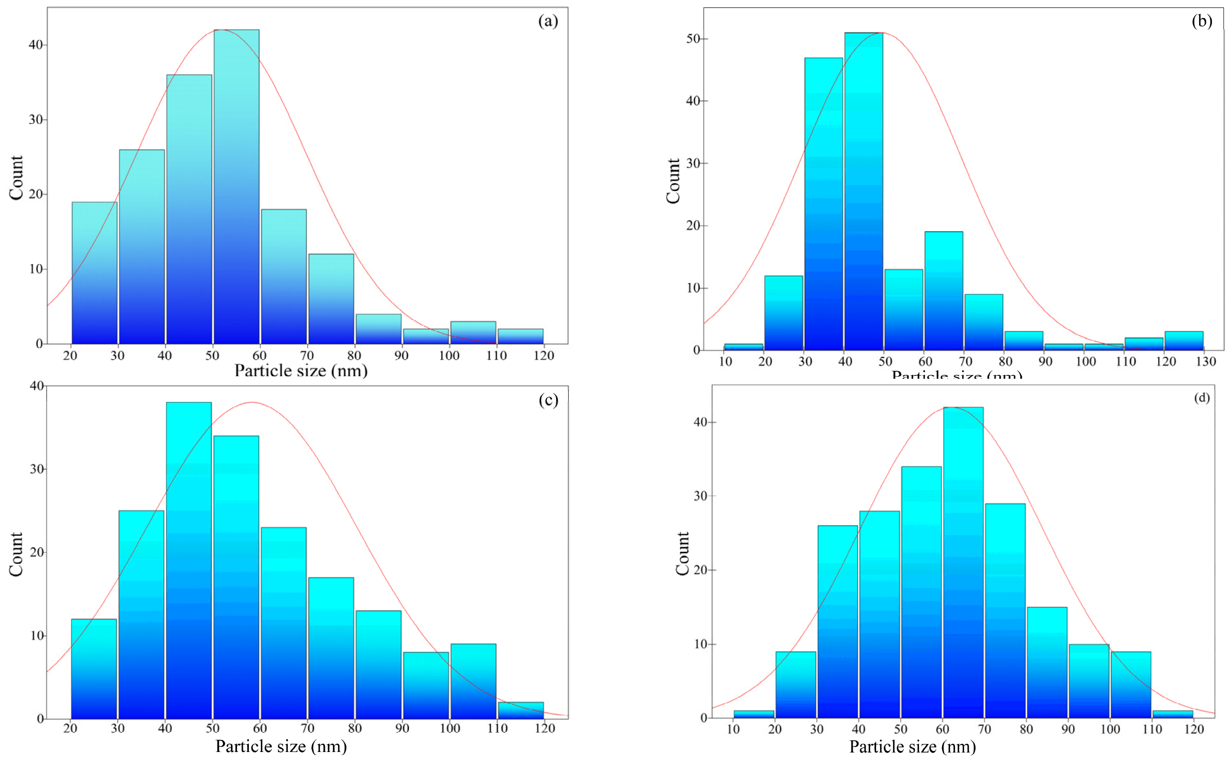


**Figure 3.** FE-SEM images of 0%, 25%, 50%, and 75% $NiFe_2O_4/TiO_2$ nanocomposites

Figure 4 presents the Raman spectra of $NiFe_2O_4/TiO_2$ nanocomposites with varying $TiO_2$ content (0%, 25%, 50%, and 75%). The Raman spectroscopy results reveal a prominent vibrational mode associated with the $TiO_2$ phase, as evidenced by the high-intensity peaks observed in the 75% $TiO_2$ sample [29]. As the $TiO_2$ content decreases, the intensity of these $TiO_2$-related peaks diminishes, highlighting the influence of $TiO_2$ concentration on the Raman signal. In contrast, the pure Ni-ferrite sample exhibits characteristic peaks at 283, 402, 469, and 689 $cm^{-1}$. These peaks shift towards lower wavelengths with increasing $TiO_2$ doping percentages, suggesting changes in the vibrational modes of the Ni-ferrite phase due to interactions with the $TiO_2$. The observed shift in peak positions and variations in peak intensities indicate a strong interaction between the Ni-ferrite and $TiO_2$ phases. This interaction likely influences the material's vibrational properties and is correlated with changes in the magnetic properties of the nanocomposites as $TiO_2$ content varies [30].

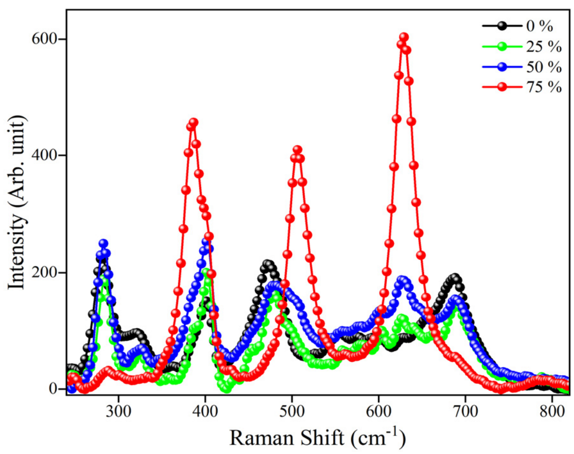


**Figure 4.** Raman spectra of 0%, 25%, 50%, and 75% $NiFe_2O_4/TiO_2$ nanocomposites

Figure 5 displays the room temperature hysteresis loops derived from Vibrating Sample Magnetometry (VSM) measurements. The magnetic properties, saturation magnetization (Ms), coercivity (Hc), and remanence magnetization ($M_R$), are summarized in Table 2.

Figure 6 presents the variation curves for Ms and $M_R$ with different $TiO_2$ concentrations. The results reveal a decline in Ms and magnetic moment ($\mu$) as $TiO_2$ content increases, indicating a systematic reduction in the magnetic properties of the $NiFe_2O_4/TiO_2$ nanocomposites. This reduction is attributed to the dilution effect caused by the incorporation of $TiO_2$, which progressively diminishes the magnetic properties of the $NiFe_2O_4$ phase [31,32]. Since $TiO_2$

is non-magnetic, its presence reduces the concentration of the magnetic $NiFe_2O_4$ phase, leading to an overall decrease in the magnetic moment of the nanocomposites. Notably, Hc remains relatively stable across different $TiO_2$ concentrations, suggesting that the incorporation of $TiO_2$ does not significantly affect the magnetic anisotropy of the nanocomposites [33,34]. The consistent coercivity indicates that $TiO_2$ does not substantially alter the magnetic domain structure or the magnetization reversal process in the $NiFe_2O_4$ phase.

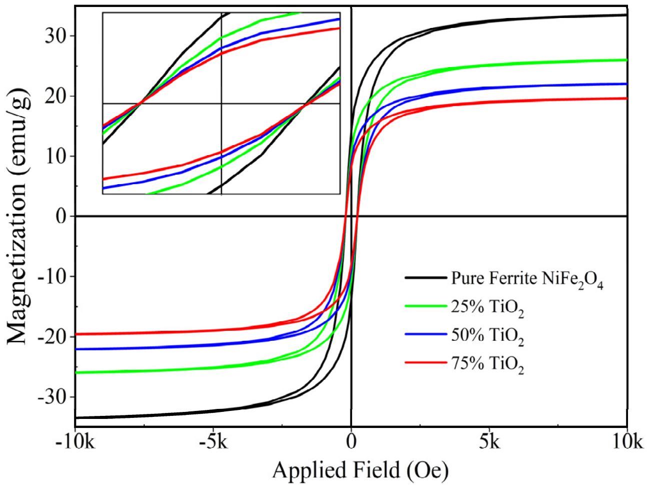


**Figure 5.** RT Magnetic curves of 0%, 25%, 50%, and 75% $NiFe_2O_4/TiO_2$ nanocomposites

**Table 2.** RT Magnetic parameters

| $TiO_2$ % | $M_S$ (emu/g) | $M_R$ (emu/g) | $H_C$ (Oe) | ηB (μB) | K×$10^3$ (emu.Oe/g) |
|---|---|---|---|---|---|
| 0 | 33.73 | 14.29 | 204.1 | 1.416 | 7.17 |
| 25 | 26.28 | 10.86 | 204.7 | 1.479 | 5.60 |
| 50 | 22.24 | 9.19 | 205.9 | 1.251 | 4.77 |
| 75 | 19.75 | 8.3 | 206.9 | 1.111 | 4.26 |

The observed decrease in saturation magnetization and magnetic moment with increasing $TiO_2$ content may also be related to changes in particle size and surface effects, as indicated by the FESEM analysis [35]. Variations in particle size and potential surface phenomena, such as increased porosity or agglomeration, could further impact the magnetic properties of the nanocomposites. These factors must be considered when interpreting the changes in magnetic behavior with varying $TiO_2$ concentrations.

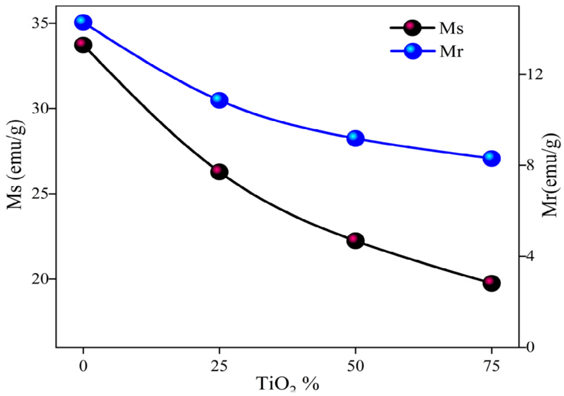


**Figure 6.** RT Magnetic Saturation (Ms) and Remanence ($M_R$) variation curves of 0%, 25%, 50%, and 75% $NiFe_2O_4/TiO_2$ nanocomposites

## 4. CONCLUSIONS

This study provides significant insights into $NiFe_2O_4/TiO_2$ nanocomposites, focusing particularly on their magnetic properties alongside structural and morphological aspects. X-ray diffraction (XRD) confirmed the successful synthesis of these nanocomposites, revealing the presence of both $NiFe_2O_4$ and $TiO_2$ phases. Field emission scanning electron microscopy (FESEM) demonstrated a uniform distribution of $TiO_2$ within the $NiFe_2O_4$ matrix, with particle size decreasing as $TiO_2$ content increased, suggesting that $TiO_2$ acts as a grain refiner. Raman spectroscopy further revealed strong interactions between $NiFe_2O_4$ and $TiO_2$, leading to changes in vibrational modes that influence the material's magnetic behavior.

The magnetic studies, conducted via Vibrating Sample Magnetometry (VSM), are particularly noteworthy. The results showed a significant decrease in saturation magnetization and magnetic moment as $TiO_2$ content increased, highlighting a pronounced dilution effect on the magnetic properties of the $NiFe_2O_4$ phase. This reduction is a direct consequence of the non-magnetic $TiO_2$ phase diluting the magnetic contribution of $NiFe_2O_4$. Despite this decrease, the coercivity remained stable across different $TiO_2$ concentrations, indicating that $TiO_2$ incorporation does not significantly affect the magnetic anisotropy or the magnetization reversal process. This stability in coercivity suggests that the fundamental magnetic characteristics of the $NiFe_2O_4$ phase are preserved, even as its magnetic moment is diluted.

Looking ahead, future research should prioritize optimizing synthesis parameters to further refine these magnetic properties, exploring different $TiO_2$ doping levels and alternative materials. Additionally, practical applications in spintronics, magnetic sensors, and catalysis could benefit from these findings, making it crucial to evaluate how these nanocomposites perform in specific technological contexts. Comparative studies with other materials will also be valuable to highlight the relative advantages of $NiFe_2O_4/TiO_2$ nanocomposites. Overall, this work advances our understanding of $TiO_2$ doping effects on $NiFe_2O_4$ nanocomposites, emphasizing their potential for applications requiring tailored magnetic properties.

**Acknowledgments**
The authors acknowledge the Physics Department, College of Education, Garmian University, for providing the facilities for the synthesis and characterization used in this study.

**Conflict of interest**
On behalf of all authors, the corresponding author states that there is no conflict of interest.

**Data access statement**
All data generated during this study are included in the manuscript.

**ORCID**
**A.K. Sijo,** https://orcid.org/0000-0002-1478-2088; **Ali M. Mohammad,** https://orcid.org/0000-0003-1659-8855
**J. Mazurenko,** https://orcid.org/0000-0002-8446-5280

**REFERENCES**

[1] H. Wang, T.N. Lamichhane, and M.P. Paranthaman, "Review of additive manufacturing of permanent magnets for electrical machines: A prospective on wind turbine," Materials Today Physics, **24**, 100675 (2022). https://doi.org/10.1016/j.mtphys.2022.100675

[2] A. Hirohata, K. Yamada, Y. Nakatani, I.L. Prejbeanu, B. Diény, P. Pirro, and B. Hillebrands, "Review on spintronics: Principles and device applications," Journal of Magnetism and Magnetic Materials, **509**, 166711 (2020). https://doi.org/10.1016/j.jmmm.2020.166711

[3] S.J. Salih, and W.M. Mahmood, "Review on magnetic spinel ferrite (MFe2O4) nanoparticles: From synthesis to application," Heliyon, **9**(6), e16601 (2023). https://doi.org/10.1016/j.heliyon.2023.e16601

[4] G. Rana, P. Dhiman, A. Kumar, D-V.N. Vo, G. Sharma, S. Sharma, and M. Naushad, "Recent advances on nickel nano-ferrite: A review on processing techniques, properties and diverse applications," Chemical Engineering Research and Design, **175**, 182-208 (2021). https://doi.org/10.1016/j.cherd.2021.08.040

[5] J. Mazurenko, A.K. Sidjo, L. Kaykan, J.M. Michalik, L. Gondek, E. Szostak, and Ż. Antoni, "Impact of cation distribution in shaping the structural and magnetic characteristics of Ni-Cu ferrite," Physica Scripta, **100**, 035940 (2025). https://doi.org/10.1088/1402-4896/adb2c3

[6] T. Dippong, E.A. Levei, and O. Cadar, "Correlation between structure, morphology and magnetic properties in ZnxCo0.8−xNi0.2Fe2O4@SiO2 (0.1÷0.7) nanocomposites," Journal of Alloys and Compounds, **938**, 168503 (2023). https://doi.org/10.1016/j.jallcom.2022.168503

[7] T. Tatarchuk, M. Bououdina, W. Macyk, *et al.* "Structural, Optical, and Magnetic Properties of Zn-Doped CoFe2O4 Nanoparticles," Nanoscale Research Letters, **12**, 141 (2017). https://doi.org/10.1186/s11671-017-1899-x

[8] P. Sahoo, P. Choudhary, S.S. Laha, A. Dixit, and O.T. Mefford, "Recent advances in zinc ferrite (ZnFe2O4) based nanostructures for magnetic hyperthermia applications," Chemical Communications, **59**, 12065-12090 (2023). https://doi.org/10.1039/D3CC01637D

[9] R. Javed, *et al*. "Diverse biotechnological applications of multifunctional titanium dioxide nanoparticles: an up-to-date review," IET Nanobiotechnology, **16**(5), 171-189 (2022). https://doi.org/10.3390/ma15051863

[10] X. Chen, W. Zhu, J. Chen, Q. Cao, Y. Chen, and D. Hu, "$TiO_2$ Nanoparticle/Polyimide Nanocomposite for Ultrahigh-Temperature Energy Storage," Nanomaterials, **12**(24), 4458 (2022). https://doi.org/10.3390/nano12244458

[11] A.A. Nassar, A.A.E.A. Elfiky, A.K. El-Sawaf, *et al*. "Sustainable green synthesis and characterization of nanocomposites for synergistic photocatalytic degradation of Reactive Orange 16 in textile wastewater using CuO@A-TiO2/Ro-TiO2," Scientific Reports, **14**, 16188 (2024). https://doi.org/10.1038/s41598-024-63294-3

[12] A.K. Sijo, V.K. Jha, L.S. Kaykan, and D.P. Dutta, "Structure and cation distribution in superparamagnetic NiCrFeO4 nanoparticles using Mössbauer study," Journal of Magnetism and Magnetic Materials, **497**, 166047 (2020). https://doi.org/10.1016/j.jmmm.2019.166047

[13] J. Mazurenko, L. Kaykan, A.K. Sijo, M. Moiseienko, M. Kuzyshyn, N. Ostapovych, and M. Moklyak, "The influence of reaction medium pH on the structure, optical, and mechanical properties of nanosized CU-FE ferrite synthesized by the Sol-Gel autocombustion method," Journal of Nano Research, **81**, 65–84 (2023). https://doi.org/10.4028/p-d2fqah

[14] A.K. Sijo, "Magnetic and structural properties of $CoCr_xFe_{2-x}O_4$ spinels prepared by solution self combustion method," Ceramics International, **43**(2), 2288-2290 (2017). https://doi.org/10.1016/j.ceramint.2016.11.010

[15] A. Varma, A.S. Mukasyan, A.S. Rogachev, and K.V. Manukyan, "Solution Combustion Synthesis of Nanoscale Materials," Chemical Reviews, **116**(23), 14493-14586 (2016). https://doi.org/10.1021/acs.chemrev.6b00279

[16] M. Ginting, S. Taslima, K. Sebayang, D. Aryanto, T. Sudiro, and P. Sebayang, "Preparation and characterization of zinc oxide doped with ferrite and chromium," AIP Conf. Proc. **1862**, 030062 (2017). https://doi.org/10.1063/1.4991166
[17] B. Jaleh, M. Kashfi, B.F. Mohazzab, "Experimental characterization and finite element investigation of SiO2 nanoparticles reinforced dental resin composite," Sci. Rep. **14**, 7794 (2024). https://doi.org/10.1038/s41598-024-58114-7
[18] Y. Li, Y. Sun, J. Wu, G. Ren, X. Xu, B. Corcoran, S.T. Chu, *et al*. "Performance Analysis of Microwave Photonic Spectral Filters based on Optical Microcombs," Advanced Photonics Research, 1(1), 2400084 (2024). https://doi.org/10.1002/apxr.202400084
[19] A.M. Mohammad, S.M.A. Ridha, and T.H. Mubarak, "Structural and magnetic properties of Mg-Co ferrite," Digest Journal of Nanomaterials and Biostructures, **13**(3), 615-623 (2018). https://chalcogen.ro/615_MohammadAM.pdf
[20] A. Sijo, and D.P. Dutta, "Size-dependent magnetic and structural properties of CoCrFeO4 nano-powder prepared by solution self-combustion," Journal of Magnetism and Magnetic Materials, **451**, 450–453 (2017). https://doi.org/10.1016/j.jmmm.2017.11.092
[21] A. Kumar, P. Sharma, and D. Varshney, "Structural, vibrational and dielectric study of Ni doped spinel Co ferrites: Co1−xNixFe2O4 (x=0.0, 0.5, 1.0)," Ceramics International, **40**(8), 12855-12860 (2014). https://doi.org/10.1016/j.ceramint.2014.04.140
[22] I. Ran, H. Liu, H. Dong, P. Gao, H. Cheng, J. Xu, H. Wang, *et al*. "Accurate quantification of TiO2(B)'s phase purity via Raman spectroscopy," Green Energy and Environment, **8**(5),1371-1379 (2023). https://doi.org/10.1016/j.gee.2022.02.008
[23] X. Liu, and J. Fu, "Electronic and elastic properties of the tetragonal anatase TiO2 structure from first principle calculation," Optik, **206**, 164342 (2020). https://doi.org/10.1016/j.ijleo.2020.164342
[24] K.R. Ramkumar, and S. Natarajan, "Effects of TiO2 nanoparticles on the microstructural evolution and mechanical properties of accumulative roll bonded Al nanocomposites," Journal of Alloys and Compounds, **793**, 526-532 (2019). https://doi.org/10.1016/j.jallcom.2019.04.218
[25] S. Kobayashi, Y. Ikuhara, and T. Mizoguchi, "Lattice expansion and local lattice distortion in Nb- and La-doped SrTiO3 single crystals investigated by x-ray diffraction and first-principles calculations," Physical Review B, **98**(13), 134114 (2018). https://doi.org/10.1103/PhysRevB.98.134114
[26] W. Qin, T. Nagase, Y. Umakoshi, and J.A. Szpunar, "Relationship between microstrain and lattice parameter change in nanocrystalline materials," Philosophical Magazine Letters, **88**(3), 169–179 (2008). https://doi.org/10.1080/09500830701840155
[27] H. Zhang, Q. Tang, Q. Li, Q. Song, H. Wu, and N. Mao, "Enhanced Photocatalytic Properties of PET Filaments Coated with Ag-N Co-Doped TiO2 Nanoparticles Sensitized with Disperse Blue Dyes," Nanomaterials, **10**(5), 987 (2020). https://doi.org/10.3390/nano10050987
[28] C. Liang, Z. Jia, and R. Chen, "An Automated Particle Size Analysis Method for SEM Images of Powder Coating Particles," Coatings, **13**(9), 1547 (2023). https://doi.org/10.3390/coatings13091547
[29] E.J. Ekoi, A. Gowen, R. Dorrepaal, and D.P. Dowling, "Characterisation of titanium oxide layers using Raman spectroscopy and optical profilometry: Influence of oxide properties," Results in Physics, **12**, 1574-1585 (2019). https://doi.org/10.1016/j.rinp.2019.01.054
[30] M.K. Kokare, N.A. Jadhav, Y. Kumar, K.M. Jadhav, and S.M. Rathod, "Effect of Nd3+ doping on structural and magnetic properties of Ni0.5Co0.5Fe2O4 nanocrystalline ferrites synthesized by sol-gel auto combustion method," Journal of Alloys and Compounds, **748**, 1053-1061 (2018). https://doi.org/10.1016/j.jallcom.2018.03.168
[31] L.S. Kaykan, J.S. Mazurenko, N.V. Ostapovych, A.K. Sijo, and N.Y. Ivanichok, "Effect of PH on structural morphology and magnetic properties of ordered phase of cobalt doped lithium ferrite nanoparticles synthesized by SoL-Gel auto-combustion method," Journal of Nano- and Electronic Physics, **12**(4), 04008–7 (2020). https://doi.org/10.21272/jnep.12(4).04008
[32] E.D. Smolensky, H.Y. Park, Y. Zhou, G.A. Rolla, M. Marjańska, M. Botta, and V.C. Pierre, "Scaling Laws at the Nano Size: The Effect of Particle Size and Shape on the Magnetism and Relaxivity of Iron Oxide Nanoparticle Contrast Agents," Journal of Materials Chemistry B, **1**(22), 2818-2828 (2013). https://doi.org/10.1039/C3TB00369H
[33] J. Mazurenko, A.K. Sidjo, L. Kaykan, J.M. Michalik, Ł. Gondek, E. Szostak, A. Żywczak, and V. Moklyak, "Magneto-Structural properties of MG-Substituted copper ferrite nanoparticles," Materials Research Express, **11**(12), 125003 (2024). https://doi.org/10.1088/2053-1591/ad9c19
[34] D. Dey, N. Halder, K.P. Misra, S. Chattopadhyay, S.K. Jain, P. Bera, N. Kumar, and A.K. Mukhopadhyay, "Systematic study on the effect of Ag doping in shaping the magnetic properties of sol-gel derived TiO2 nanoparticles," Ceramics International, **46**(17), 27832-27848 (2020). https://doi.org/10.1016/j.ceramint.2020.07.282

## ПРОЕКТУВАННЯ ТА РОЗРОБКА НАНОКОМПОЗИТІВ ФЕРИТ-$TiO_2$ З НАСТРОЮВАНИМИ МАГНІТНИМИ ВЛАСТИВОСТЯМИ

**Ханаа Ш. Ахмед[1], А.К. Сіджо[2], Алі М. Мохаммад[1], Геро С. Ахмед Аль-Джаф[1], Бален Х. Ахмед[1], Ю. Мазуренко[3]**
*[1]Університет Гарміана, Коледж освіти, Кафедра фізики, Курдистан, Калар-46021, Ірак*
*[2]Кафедра фізики, Коледж мистецтв та наук імені Мері Матха, Манантаваді, Університет Каннур-670645, Індія*
*[3]Кафедра медичної інформатики, Івано-Франківський національний медичний університет, вул. Галицька, 2, 76018, Івано-Франківськ, Україна*

Нанокомпозити Ni-ферит-$TiO_2$ з різним вмістом $TiO_2$ (0%, 25%, 50% та 75%) були синтезовані за допомогою методу золь-гель автогоріння та охарактеризовані за допомогою рентгенівської дифракції (XRD), FE-SEM, VSM та раманівської спектроскопії. Рентгенівський дифракціональний аналіз підтвердив співіснування фаз фериту та $TiO_2$. Зображення FE-SEM показали рівномірний розподіл частинок та зменшення розміру частинок зі збільшенням вмісту $TiO_2$. Раманівська спектроскопія продемонструвала сильні коливальні моди, пов'язані з $TiO_2$, причому найвища інтенсивність спостерігалася у зразку з 75% $TiO_2$, зменшуючи її зі зменшенням вмісту $TiO_2$. Піки, що спостерігалися в чистому Ni-фериті (283, 402, 469 та 689 $см^{-1}$), зміщувалися до нижчих довжин хвиль зі збільшенням легування $TiO_2$, що вказує на змінені коливальні моди через фазові взаємодії. Ці взаємодії, ймовірно, сприяли змінам магнітних властивостей. Аналіз VSM виявив зменшення намагніченості насичення та залишкової магнітної напруги зі збільшенням вмісту $TiO_2$, тоді як коерцитивна сила залишалася стабільною. Магнітна поведінка була пов'язана з розведенням $TiO_2$ та межами розділу фаз, що дає цінні знання для розробки магнітних матеріалів з індивідуальними властивостями.

**Ключові слова:** *ферит; нанокомпозити; магнітні властивості; наночастинки; гібридний ферит*